

## Journal Pre-proofs

Highly regioselective and stereoselective photodimerization of azine-containing stilbenes in neat condition: An efficient synthesis of novel cyclobutanes with heterocyclic substituents

Alina E. Saifutiarova, Yuri V. Fedorov, François Maurel, Elena N. Gulakova, Valentina A. Karnoukhova, Olga A. Fedorova

PII: S1010-6030(22)00036-3  
DOI: <https://doi.org/10.1016/j.jphotochem.2022.113804>  
Reference: JPC 113804

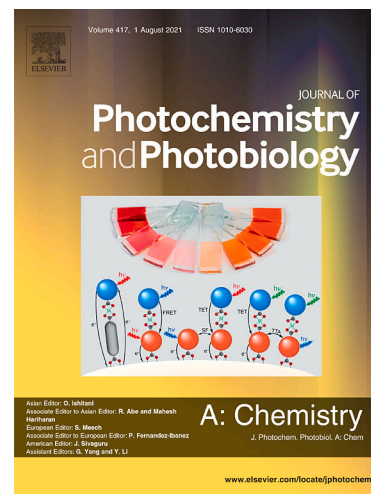
To appear in: *Journal of Photochemistry & Photobiology, A: Chemistry*

Received Date: 6 December 2021  
Revised Date: 11 January 2022  
Accepted Date: 14 January 2022

Please cite this article as: A.E. Saifutiarova, Y.V. Fedorov, F. Maurel, E.N. Gulakova, V.A. Karnoukhova, O.A. Fedorova, Highly regioselective and stereoselective photodimerization of azine-containing stilbenes in neat condition: An efficient synthesis of novel cyclobutanes with heterocyclic substituents, *Journal of Photochemistry & Photobiology, A: Chemistry* (2022), doi: <https://doi.org/10.1016/j.jphotochem.2022.113804>

This is a PDF file of an article that has undergone enhancements after acceptance, such as the addition of a cover page and metadata, and formatting for readability, but it is not yet the definitive version of record. This version will undergo additional copyediting, typesetting and review before it is published in its final form, but we are providing this version to give early visibility of the article. Please note that, during the production process, errors may be discovered which could affect the content, and all legal disclaimers that apply to the journal pertain.

© 2022 Elsevier B.V. All rights reserved.



# Highly regioselective and stereoselective photodimerization of azine-containing stilbenes in neat condition: An efficient synthesis of novel cyclobutanes with heterocyclic substituents

Alina E. Saifutiarova <sup>a,\*</sup>, Yuri V. Fedorov <sup>a</sup>, François Maurel<sup>b</sup>, Elena N. Gulakova <sup>a</sup>,  
Valentina A. Karnoukhova <sup>a</sup>, Olga A. Fedorova <sup>a</sup>

<sup>a</sup>*A. N. Nesmeyanov Institute of Organoelement Compounds of Russian Academy of Sciences,  
119991, Vavilova str., 28, Moscow, Russia*

<sup>b</sup>*Université de Paris, ITODYS, CNRS, F-75006 Paris, France*

\* Corresponding author. E-mail addresses: baykova.alina@gmail.com (A.E. Saifutiarova), fedorova@ineos.ac.ru (O.A. Fedorova).

## Abstract.

We have developed a visible light promoted reaction of intermolecular [2 + 2] cycloaddition of heterostilbene molecules containing a phenyl ring with OMe donor groups and a 6-membered nitrogen-containing ring as an acceptor, which proceeds under mild conditions in water at room temperature. The corresponding cyclobutane derivatives were synthesized with yields of up to 57%. The efficiency of this photoreaction depends on the nature of the heterocyclic residue and the concentration of heterostilbenes. The mild reaction conditions and the absence of additives facilitate the reaction. This work provides a convenient and gentle method for the preparation of cyclobutanes.

**Key words.** heterostilbene; intermolecular [2 + 2] photocycloaddition; cyclobutane; photoreaction; regioselectivity; stereoselectivity.

## 1 Introduction

Recently particular attention has been paid to such derivatives as cyclobutanes, which are quite important synthetic products that provide a one-step transition from simple molecules to more complex ones, and play an important role in the synthesis of natural products and other complex structures [1,2]. As pointed out with several excellent natural examples, dimerization leads to effective utilization of chemical space; therefore, such natural products provide a highly effective route for medicines compared to chemical synthesis [3]. Most of the natural derivatives of cyclobutane demonstrate remarkable biological activity; therefore, their preparation is promising for the creation of new anticancer, antibacterial and fungicidal drugs [4–7]. Cyclobutane compounds derived from chalcones or resveratrol with the resorcinol pattern, can provide HSP90,

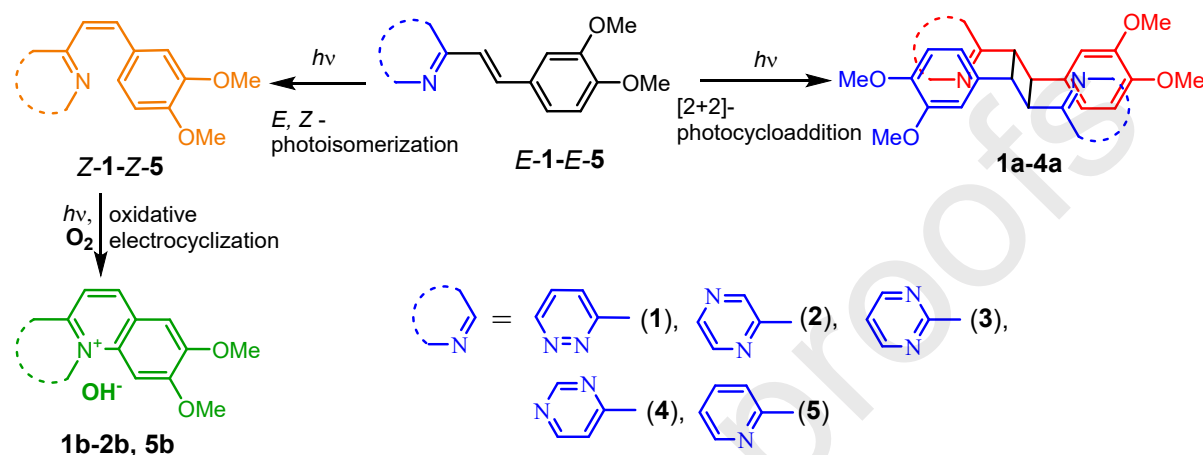
topoisomerase inhibitors and function as MDK agents and need to be explored [8]. The control of cyclobutane interaction with DNA is also being actively studied [9].

The photochemical symmetry-allowed [2+2]-cycloaddition of substituted ethenes offers a variable method for the synthesis of substituted cyclobutanes. However, when performed in solution, the dimerization unavoidably results in the formation of inseparable or poorly separable stereoisomers due to the various possible mutual orientations in the transition state and the photochemically induced *trans-cis* isomerization of the substrates. [10]

Currently, many different strategies for the formation of cyclobutane derivatives have been developed, in which the transformation can be carried out both in the solid state [11,12], and in solution [13]. In recent years, supramolecular chemistry has become an effective strategy for the controlled formation of cyclobutanes in solution via [2 + 2] photodimerization reactions [14–20]. Molecular containers such as cucurbit[n]urils [21], cyclodextrins [22,23] and self-organizing coordination cells [24] are used. All this can provide isolated cavities in which the two encapsulated olefins can be pre-oriented, resulting in the formation of stereoselective cyclobutane derivatives. Consequently, regioselective photodimerization in the neat condition remains a complex problem requiring the development of an accessible synthetic approach to cyclobutane derivatives with various substituents.

Heterostilbene molecules (HST) are well-developed class of the olefins [25]. They can participate in the three types of the photochemical reactions, namely, *E,Z*-photoisomerization, photodimerization and photochemical intramolecular cyclization (Scheme 1). The way of the photochemical transformation can be controlled by structure of heterostilbenes [20] and the condition of their photolysis. In this work, we present the study of the photochemical reactions of azine-containing stilbenes *E-1-E-5* (Scheme 1) aimed to find regioselective and stereoselective formation of cyclobutane derivative in solution. A strategy for constructing of cyclobutane derivatives is to provide the dimer pre-organization of HST molecules in solution, the key point of the strategy was the applying of the polar molecules for dimer pre-organization. In our case, the heterostilbenes possess donor OMe groups in phenyl ring and acceptor 6-membered nitrogen containing ring, the synthesis of the compounds were described earlier [26]. Such structural feature can lead to the arrangement of stilbene molecules in *head-to-tail* manner in appropriate solution. We speculated that the photocycloaddition reaction was significantly affected by solvent probably due to the following possible causes: a) solvent affects the excited state of heterostilbene to increase the lifetime; b) solvent effects on the dimer pre-organization of heterostilbenes. To find the conditions of cyclobutane formation the type of azine heterocycle fragment, concentration of heterostilbene in solution and type of the solvent (MeCN and water) have been varied. Pyridazin-2-yl (**1**), pyrazin-2-yl (**2**), pyrimidin-2-yl (**3**), pyrimidin-6-yl (**4**), and pyridine-2-yl (**5**) were used

as heterocyclic nuclei. We also studied the ground state properties and photoreactivities of these compounds *E-1* and *E-5* with theoretical approaches in the frame of Density Functional Theory (DFT and TD-DFT calculations). Theoretical calculations have been performed to gain insight into the photophysical properties of two compounds demonstrated different behavior when illuminated by light.



**Scheme 1.** Photochemical transformations of heterostilbene molecules, and structures of the studied compounds.

## 2 Experimental

### Materials and methods

All reagents and solvents were obtained from commercial sources and used as received. For the spectroscopic (UV/Vis and fluorescence) studies, MeCN and water from a Milli-Q ultrapure water system were used.

#### 2.1. Physical measurements

$^1\text{H-NMR}$  spectra were recorded in  $\text{CD}_3\text{CN}$  and  $\text{CD}_3\text{COCD}_3$  on a Bruker 400 and 600 MHz, and  $^{13}\text{C}$  NMR spectra were recorded at 101 or 151 MHz at ambient temperature using 5 mm tubes. Chemical shifts were determined with accuracy of 0.01 and 0.1 ppm for  $^1\text{H}$  and  $^{13}\text{C}$  spectra, respectively, and are reported relative to the residual signal of the solvent that was used as an internal standard. Spin-spin coupling constants for the proton spectra were determined with accuracy of 0.1 Hz. The  $^1\text{H}$  NMR signal assignments were performed using COSY and NOESY 2D NMR techniques. The  $^{13}\text{C}$  NMR signal assignments were performed by means of HSQC and HMBC 2D NMR techniques.  $^1\text{H}$  NMR experiments were performed using the gradient version of the WATERGATE pulse sequence. The spectra (averaged 32 scans) were acquired with 32K complex points over a spectral width of 15000 Hz ( $D19 = 100 \mu\text{s}$ , nulls at 14.7, 4.7, and -5.3 ppm). The data were processed using MestReNova version 12.0.0 on a PC workstation using Windows 10.

The reaction course and purity of the final products were determined by TLC on silica gel (DC-Fertigfolien ALUGRAM Xtra SIL60 G/UV254, MACHEREY-NAGEL) and eluent: hexane, EtOAc. Column chromatography was conducted over silica gel (Kieselgel, particle size 40–60  $\mu\text{m}$ , 60  $\text{\AA}$ , Acros Organics) on a Biotage Isolera Prime flash chromatograph.

Analysis of reaction mixtures by HPLC was carried out on a Dionex UltiMate 3000 chromatograph controlled by the Chromeleon 7 software, using Diasorb-130-C18T columns (C-18 sorbent, grain size 7  $\mu\text{m}$ , column size 4.6  $\times$  260 mm). A mixture of MeCN and H<sub>2</sub>O was used as an eluent.

Electrospray ionization mass spectrometry (ESI-MS) analyses were performed using a Finnigan LCQ Advantage mass spectrometer equipped with an octopole ion-trap mass-analyzer, an MS Surveyor pump, a Surveyor auto sampler, a Schmidlin-Lab nitrogen generator (Germany), and Finnigan X-Calibur 1.3 software for data collecting and processing. High resolution mass spectra were recorded on a time-of-flight instrument in a positive-ion mode using ESI method.

Melting points were measured in capillaries on a Mel-temp II instrument and were not corrected.

Elemental analysis was performed on a Carlo Erba 1108 elemental analyzer.

### 2.1.2. Steady-state optical measurements

Preparation and handling of the solutions were carried out under red light. Registration of electronic absorption spectra under continuous irradiation of the samples was carried out using a high-speed fiber-optic spectrophotometer "AvaSpec-2048-USB2, Avantes BV". Fluorescence spectra were measured on a Cary Eclipse spectrofluorometer (Agilent). Varian-Cary 300 spectrophotometer was used to measure electronic absorption spectra. The spectral measurements were carried out in air-saturated acetonitrile or water solutions at  $20 \pm 1$  °C; the concentrations of the studied compounds were in the range  $2 \cdot 10^{-5}$  M -  $2 \cdot 10^{-2}$  M.

The light intensity was measured by a Nova P/N 7Z01500 power meter equipped with a 3A-FS P/N 7Z02628 thermal power/energy measurement sensor. The photochemical transformations were induced by irradiation of acetonitrile or aqueous solutions of compounds **1-5** with a high pressure mercury lamp (DRK-120, 120 W). The particular lines of the mercury lamp spectrum with  $\lambda = 313, 365,$  and  $405$  nm were isolated by glass filters from the standard set of colored optical glasses. The photo-processes were studied in a 10 mm quartz cell with stirring.

For obtaining the spectra of the Z-isomers of dyes **1-5** by Fischer's method, the solutions were irradiated at  $\lambda = 313$  and  $365$  nm until the photostationary states were attained [24].

Quinine bisulfate in 1N sulfuric acid ( $\phi^{\text{fl}} = 55.0\%$ ) [27] were used as a reference for the fluorescence quantum yield measurements. The fluorescence quantum yields [28] were calculated using equation:

$$\varphi^{fl} = \varphi_0^{fl} \frac{S_i \cdot (1 - 10^{-A_0}) \cdot n_i^2}{S_0 \cdot (1 - 10^{-A_i}) \cdot n_0^2},$$

where  $\varphi_i$  and  $\varphi_0$  are the fluorescence quantum yields of the studied solution and the standard compound, respectively;  $A_i$  and  $A_0$  are the absorptions of the studied solution and the standard, respectively;  $S_i$  and  $S_0$  are the areas underneath the curves of the fluorescence spectra of the studied solution and the standard, respectively; and  $n_i$  and  $n_0$  are the refractive indices of the solvents for the substance under study and the standard compound ( $n_i = 1.333$ , water;  $n_i = 1.34$ , acetonitrile;  $n_0 = 1.397$ , 1N sulfuric acid).

Photochemical reactions were carried out with a high-pressure Hg vapor lamp (120 W) and an immersed Hg photoreactor (125 W). Electronic absorption spectra were measured on a fiber-optic spectrophotometer connected to a computer at  $20 \pm 1$  °C.

The quantum yield of the backward photocycloaddition reaction was determined by analyzing the kinetics of spectral changes upon irradiation of  $3.0 \times 10^{-5}$  M solution of cyclobutane **7** in water with 313 nm light. During the fitting procedure using the Sa3.3 program, the quantum yields of the backward reaction of *E-Z* photoisomerization of dye **2** were fixed as known.

## 2.2. Synthesis of compounds

### 2.2.1. Synthesis of compounds **1-5**.

Synthesis of (E)-3-(3,4-dimethoxystyryl)pyridazine (**1**), (E)-2-(3,4-dimethoxystyryl)pyrazine (**2**), (E)-2-(3,4-dimethoxystyryl)pyrimidine (**3**), (E)-4-(3,4-dimethoxystyryl)pyrimidine (**4**) has been described in [19] and (E)-2-(3,4-dimethoxystyryl)pyridine (**5**) has been described in [29].

### 2.2.2. General procedure for the preparation of [2+2]-photocycloaddition products **1a-4a**.

Solution of **1-4** in water ( $10^{-2}$  M) was irradiated with unfiltered light of high-pressure mercury lamp for 23h in 5 mm NMR tubes. The precipitate formed during the reaction was washed with water and isolated:

**3,3'**-**(2,4-bis(3,4-dimethoxyphenyl)cyclobutane-1,3-diyl)dipyridazine (1a)**, yield 6.3 mg (57%), m.p. 88-90°C.  $^1\text{H NMR}$  ( $\text{CDCl}_3$ , 600 MHz, 25 °C): 3.75 (s, 6H,  $\text{OCH}_3$ ), 3.79 (s, 6H,  $\text{OCH}_3$ ), 4.80 (m, 2H, H-a, H-a'), 5.30 (m, 2H, H-b, H-b'), 6.66 (s, 2H, H-2, H-2'), 6.66-6.68 (d, 2H, H-5, H-5'), 3J = 8.4), 6.82-6.84 (d, 2H, H-6, H-6', 3J = 8.1), 7.14-7.15 (d, 2H, H-10, H-10', 3J = 7.9), 7.27 (t, 2H, H-11, H-11'), 9.00 (s, 2H, H-12, H-12');  $^{13}\text{C NMR}$  ( $\text{CDCl}_3$ , 151 MHz, 25 °C)  $\delta$ : 44.2 (2C, C-a, C-a'), 48.1 (2C, C-b, C-b'), 55.7 (2C,  $\text{OCH}_3$ ), 55.9 (2C,  $\text{OCH}_3$ ), 110.8 (2C, C-5, C-5'), 111.4 (2C, C-2, C-2'), 120.4 (2C, C-6, C-6'), 126.7 (2C, C-10, C-10'), 128.2 (2C, C-9, C-9'), 131.5 (2C, C-1, C-1'), 147.7 (2C, C-4, C-4'), 148.6 (2C, C-3, C-3'), 149.2 (4C, C-8, C-8', C-11, C-11'). Elemental analysis: calculated (%) for  $\text{C}_{28}\text{H}_{28}\text{N}_4\text{O}_4$  (MW 484.55): C, 69.41; H, 5.82; N, 11.56;

found C, 69.22; H, 5.50; N, 12.05. ESI-MS **1a** in MeCN, m/z: calcd 484.55; found 485.35 [**1a** + H]<sup>+</sup>, 486.40 [**1a** + H]<sup>2+</sup>

**2,2'**-**(2,4-bis(3,4-dimethoxyphenyl)cyclobutane-1,3-diyl)dipyrazine (2a)**, yield 6.0 mg (50%), m.p. 90-93°C. <sup>1</sup>H NMR (CDCl<sub>3</sub>, 600 MHz, 25 °C): 3.74 (s, 6H, OCH<sub>3</sub>), 3.80 (s, 6H, OCH<sub>3</sub>), 4.71 (dd, 2H, H-a, H-a', 3J = 9.9, 3J = 7.2), 4.91 (dd, 2H, H-b, H-b', 3J = 9.9, 3J = 7.3), 6.59 (s, 2H, H-2, H-2'), 6.68-6.69 (d, 2H, H-5, H-5', 3J = 8.2), 6.76-6.78 (d, 2H, H-6, H-6', 3J = 8.3), 8.29 (d, 2H, H-12, H-12', 3J = 2.6), 8.33 (s, 2H, H-9, H-9'), 8.48 (s, 2H, H-11, H-11'); <sup>13</sup>C NMR (CDCl<sub>3</sub>, 151 MHz, 25 °C) δ: 44.3 (2C, C-a, C-a'), 49.9 (2C, C-b, C-b'), 55.7 (4C, OCH<sub>3</sub>), 110.4 (2C, C-5, C-5'), 111.3 (2C, C-2, C-2'), 119.9 (2C, C-6, C-6'), 131.6 (2C, C-1, C-1'), 141.9 (2C, C-12, C-12'), 143.8 (2C, C-11, C-11'), 145.1 (2C, C-9, C-9'), 147.6 (2C, C-4, C-4'), 148.6 (2C, C-3, C-3'), 155.8 (2C, C-8, C-8'). Elemental analysis: calculated (%) for C<sub>28</sub>H<sub>28</sub>N<sub>4</sub>O<sub>4</sub> (MW 484.55): C, 69.41; H, 5.82; N, 11.56; found C, 69.84; H, 5.60; N, 11.53. ESI-MS **2a** in MeCN, m/z: calcd 484.55; found 485.35 [**2a** + H]<sup>+</sup>, 486.45 [**2a** + H]<sup>2+</sup>, 488.40 [**2a** + H]<sup>4+</sup>.

**2,2'**-**(2,4-bis(3,4-dimethoxyphenyl)cyclobutane-1,3-diyl)dipyrimidine (3a)**, yield 4.0 mg (40%), m.p. 100-102°C. <sup>1</sup>H NMR (CDCl<sub>3</sub>, 600 MHz, 25 °C): 3.76 (s, 6H, OCH<sub>3</sub>), 3.79 (s, 6H, OCH<sub>3</sub>), 4.90 (dd, 2H, H-a, H-a', 3J = 10.2, 3J = 7.2), 5.04 (dd, 2H, H-b, H-b', 3J = 10.2, 3J = 7.1), 6.65-6.67 (d, 2H, H-5, H-5', 3J = 8.2), 6.71 (s, 2H, H-2, H-2'), 6.82-6.84 (d, 2H, H-6, H-6', 3J = 8.3), 7.01 (t, 2H, H-11, H-11'), 8.58-8.59 (d, 4H, H-10, H-10', H-12, H-12', 3J = 2.6); <sup>13</sup>C NMR (CDCl<sub>3</sub>, 151 MHz, 25 °C) δ: 44.7 (2C, C-a, C-a'), 46.5 (2C, C-b, C-b'), 55.7 (4C, OCH<sub>3</sub>), 110.4 (2C, C-5, C-5'), 111.3 (2C, C-2, C-2'), 118.4 (2C, C-11, C-11'), 119.9 (2C, C-6, C-6'), 132.5 (2C, C-1, C-1'), 147.2 (2C, C-4, C-4'), 148.2 (2C, C-3, C-3'), 156.6 (4C, C-10, C-10', C-12, C-12'), 169.5 (2C, C-8, C-8'). Elemental analysis: calculated (%) for C<sub>28</sub>H<sub>28</sub>N<sub>4</sub>O<sub>4</sub> (MW 484.55): C, 69.41; H, 5.82; N, 11.56; found C, 69.38; H, 5.78; N, 11.83. ESI-MS **3a** in MeCN, m/z: calcd 484.55; found 485.40 [**3a** + H]<sup>+</sup>.

**4,4'**-**(2,4-bis(3,4-dimethoxyphenyl)cyclobutane-1,3-diyl)dipyrimidine (4a)**, yield 4.0 mg (35%), m.p. 95-97°C. <sup>1</sup>H NMR (CDCl<sub>3</sub>, 400 MHz, 25 °C): 3.76 (s, 6H, OCH<sub>3</sub>), 3.80 (s, 6H, OCH<sub>3</sub>), 4.58 (dd, 2H, H-a, H-a', 3J = 9.9, 3J = 7.4), 4.90 (dd, 2H, H-b, H-b', 3J = 10.1, 3J = 7.3), 6.63 (s, 2H, H-2, H-2'), 6.67-6.69 (d, 2H, H-5, H-5', 3J = 7.8), 6.75-6.77 (d, 2H, H-6, H-6', 3J = 8.6), 6.98 (t, 2H, H-11, H-11', 3J = 5.4), 8.43-8.44 (d, 2H, H-12, H-12', 3J = 5.4), 9.12 (s, 2H, H-8, H-8'); <sup>13</sup>C NMR (CDCl<sub>3</sub>, 101 MHz, 25 °C) δ: 44.5 (2C, C-a, C-a'), 48.8 (2C, C-b, C-b'), 55.8 (4C, OCH<sub>3</sub>), 110.8 (2C, C-5, C-5'), 111.5 (2C, C-2, C-2'), 119.9 (2C, C-6, C-6'), 131.3 (2C, C-1, C-1'), 147.6 (2C, C-3, C-3'), 148.6 (2C, C-4, C-4'), 155.8 (2C, C-12, C-12'), 158.2 (2C, C-8, C-8'), 168.6 (2C, C-10, C-10'). Elemental analysis: calculated (%) for C<sub>28</sub>H<sub>28</sub>N<sub>4</sub>O<sub>4</sub> (MW 484.55): C, 69.41; H, 5.82; N, 11.56; found C, 69.57; H, 5.90; N, 11.71. ESI-MS **4a** in MeCN, m/z: calcd 484.55; found 487.50 [**4a** + H]<sup>3+</sup>.

Synthesis of 8,9-dimethoxyimidazo[1,6-a]quinolin-11-ium perchlorate (**1b**) and 8,9-dimethoxypyrazino[1,2-a]quinolin-11-ium perchlorate (**2b**) has been described in [26], 8,9-dimethoxybenzo-[c]quinolizinium derivative **5b** has been described in [29].

### 2.3. X-ray crystallographic data and refinement details.

Single crystals of **1a** and **3a** were grown from saturated methanol solutions by slow evaporation of the solvent. X-ray diffraction data for **1a** were collected at the “XSA/Belok” station ( $\lambda = 0.79312$  Å) of the Kurchatov synchrotron radiation source [30], with a Rayonix SX-165 CCD detector. In total, 180 frames were taken using direct geometry ( $\theta = 0^\circ$ ) with an oscillation range of  $1^\circ$  in the  $\phi$  scanning mode in different orientations relative to the direction of the photon beam. Data reduction and empirical absorption correction were performed with the XDS [31] program package. Data collection for sample **3a** was performed on a Bruker SMART APEX II diffractometer equipped with a Photon-II area-detector and a graphite monochromator for MoK $\alpha$  radiation ( $\lambda = 0.71073$  Å, phi and omega scans). Frames were integrated using the Bruker SAINT software package [32] by a narrow-frame algorithm. A semiempirical absorption correction was applied with the SADABS [33] program using the intensity data of equivalent reflections. The structures **1a** and **3a** were solved using the SHELXT [34] program and refined by the full-matrix least-squares technique against F<sup>2</sup>hkl in anisotropic approximation for non-hydrogen atoms with SHELXL [35] program. Hydrogen atoms were placed in calculated positions and refined in the riding model with Uiso(H) = 1.5Ueq(Cm) for methyl groups and 1.2Ueq(Ci) for other carbon atoms to which corresponding H atoms are bonded. The structure **1a** was refined as an inversion twin with calculated BASF parameter equal to 0.50 and an extinction coefficient equal to 0.14. The cyclobutane fragment in **1a** is disordered by two positions with relative occupancies 0.9:0.1; the minor component was refined isotropically. The whole molecule in **3a** is disordered by two positions with relative occupancies 0.9:0.1; the minor component was refined isotropically with a common Uiso value and SAME instruction applied. Detailed crystallographic information is given in Table S1. CCDC 2123240-2123241 contain supplementary crystallographic data for this paper. The data can be obtained free of charge from The Cambridge Crystallographic Data Centre via [www.ccdc.cam.ac.uk/structures](http://www.ccdc.cam.ac.uk/structures).

### 2.4. Quantum chemical calculations

All calculations have been performed with the Gaussian 16, Revision B.01 [36] using default procedures, algorithms and integration grids. Ground state geometry optimizations of the isomers of *E-1* and *E-5* were performed using density functional theory (DFT) with the PBE0 [37] functional and the 6-311G(d,p) basis set. Molecular structures were confirmed to be real minima

or a transition state on the potential energy surface by subsequent calculation of harmonic vibrational frequencies at the same level of theory. The minima structures showed positive force constants for all normal modes of vibration while the transition indicated only one negative force constant along the reaction coordinate.

Molecular excitation energies were calculated using TD-DFT (time-dependent density functional theory) with and without the Tamm–Dancoff approximation (TDA) [38]. We performed a functional test on the absorption properties of E5 and E1) with B3LYP, PBE0 [37], M062X [39],  $\omega$ B97XD [40] and CAM-B3LYP [41] functionals. The corresponding results are presented in Table S2 and Table S3, respectively. A comparison of the calculated results with the experimental data for clearly suggests that PBE0 has better performance in terms of its closest peak position to the experimental one. Thus, all absorption spectra and emission properties were calculated at PBE0/6-311G(d,p) level. The absorption spectra were plotted using GaussSum program [42] with the full width at half maximum set as 0.2 eV. For the S2 geometries the time-dependent density functional theory (TD-DFT) was applied. Meanwhile, the integral equation formalism polarizable continuum model (IEFPCM) [43,44] was always used to simulate the solvent (acetonitrile).

## Results and discussion

Compounds **1-5** were prepared according to Scheme 1 as *E*-isomers, according to the spin-spin coupling constants of the double bond protons Ha and Hb,  $^3J = 15-16$  Hz (Figs. S1-S5 in Electronic Supporting Information (ESI)).

### *Optical characteristics*

The UV/Vis spectra of **1-5** in aqueous or acetonitrile solutions are characterized by intense long wavelength absorption bands centered at 330-350 nm which can be assigned to an efficient intramolecular charge transfer from the methoxy group to the heterocyclic rings. The absorption bands at about 245 nm correspond to the electronic transitions in the heterocyclic and phenyl fragments of **1-5** (Figure 1). The long wavelength absorption band of the 2-pyridine derivative **5** is shifted hypsochromically as compared to compounds **2-4** in accordance with the more acceptor character of the heterocyclic rings containing two nitrogen atoms (Table 1) [45].

Fluorescence characteristics of *E-1 – E-5* measured in acetonitrile or aqueous solutions are presented in Table 1. Fluorescence quantum yields of *E-1 – E-5* are low in acetonitrile, and compounds *E-1 – E-3* do not fluoresce in aqueous solution indicating that the efficient stabilization of the polar excited state increases the probability of the photochemical conversion in competition with the emission.

**Table 1.** Optical and photochemical characteristics of compounds **1-5** and **1a-4a**.

| Samples   | $\lambda_{\text{abs}}$ , nm |       | $\Phi_{E-Z}/\Phi_{Z-E}$ |           | $\lambda_{\text{fl}}$ , nm | $\Phi_{\text{fl}}$ | $\lambda_{\text{fl}}$ , nm | $\Phi_{\text{fl}}$ | $\Phi_{\text{retro-photo}}^{\text{retro-}}_{\text{photo}}^{\text{cycloaddition}}$ |              | Yield of <b>1a-4a</b> in water, % |
|-----------|-----------------------------|-------|-------------------------|-----------|----------------------------|--------------------|----------------------------|--------------------|---|--------------|-----------------------------------|
|           | MeCN                        | water | MeCN                    | water     | MeCN                       |                    | water                      |                    | MeCN  | water        |                                   |
| <b>1</b>  | 330                         | 332   | 0.07/<br>0.16           | - / -     | 460 <sup>a</sup>           | <0.001             | -                          | 0                  | -   | -            | -                                 |
| <b>2</b>  | 350                         | 348   | 0.45/<br>0.41           | - / -     | 468 <sup>b</sup>           | 0.18               | -                          | 0                  | -   | -            | -                                 |
| <b>3</b>  | 334                         | 333   | 0.83/<br>0.08           | 0.43/0.45 | 430 <sup>b</sup>           | 0.004              | -                          | 0                  | -   | -            | -                                 |
| <b>4</b>  | 346                         | 346   | 0.29/<br>0.41           | 0.36/0.54 | 455 <sup>b</sup>           | 0.012              | 505                        | 0.021              | -   | -            | -                                 |
| <b>5</b>  | 332                         | 330   | 0.60/<br>0.40           | 0.54/0.28 | 410 <sup>b</sup>           | 0.018              | 461                        | 0.014              | -   | -            | -                                 |
| <b>1a</b> | 276                         | 282   | -                       | -         | -                          | -                  | -                          | -                  | <sup>c</sup>  | <sup>c</sup> | 57                                |
| <b>2a</b> | 274                         | 274   | -                       | -         | -                          | -                  | -                          | -                  | <sup>c</sup>  | 0.002        | 50                                |
| <b>3a</b> | 282                         | 282   | -                       | -         | -                          | -                  | -                          | -                  | <sup>c</sup>  | <sup>c</sup> | 40                                |
| <b>4a</b> | 282                         | 280   | -                       | -         | -                          | -                  | -                          | -                  | 0.007   | 0.04         | 35                                |

<sup>a</sup>  $\lambda_{\text{ex}} = 330$  nm; <sup>b</sup>  $\lambda_{\text{ex}} = 340$  nm; <sup>c</sup> the quantum yield has not been determined.

### ***Photochemical transformations***

#### ***E-Z-photoisomerization***

Irradiation of the acetonitrile solutions of stilbene derivatives **E-1** – **E-5** at concentration  $3 \cdot 10^{-5}$  M with filtered light ( $\lambda = 365$  nm) of high pressure mercury lamp resulted in the decrease of the absorption intensities along with a slight blue shift of the absorption maxima that is indicative for the formation of photostationary mixtures of *E*- and *Z*-isomers of **1-5** (Scheme 1, Fig. 1a). The spectral changes observed upon irradiation with light in acetonitrile and water solutions are presented in Figs S24-S33 in ESI. The irradiation of the compounds **E-1-E-5** in acetonitrile results in the decrease of absorption intensity and small hypsochromic shift of long wavelength band (Figs. S24, S26, S28, S30, S32 in ESI). The irradiation of water solution of heterostilbenes causes small spectral changes (Figs. S25, S27, S29, S31, S33 in ESI). The observed spectral changes upon the photolysis at 313nm and 365nm light were used for calculations of quantum yields of *E-Z*-isomerization by Fischer's method (see Experimental part). Compounds **E-3-E-5** demonstrated high quantum yields of direct and back *E-Z*-isomerization in both water and acetonitrile solutions (Table 1). In aqueous solutions, in the case of compounds **E-1** and **E-2**, the spectral changes observed upon irradiation turned out to be minimal, which made it impossible to determine the quantum yields of photoisomerization in water for these compounds (Table 1, Fig. 1b and Figs S27, S29, S31, S33 in ESI).

The NMR observations confirm the formation of photostationary mixtures of *E*- and *Z*-isomers of **1-5** in acetonitrile, according to obtained spin-spin coupling constants of the double

bona protons Ha and Hb,  $^3J = 15-16$  Hz for *E*-isomers, and  $^3J = 12-13$  Hz for *Z*-isomers (see for example Figs. S1-S5, S57 in ESI).

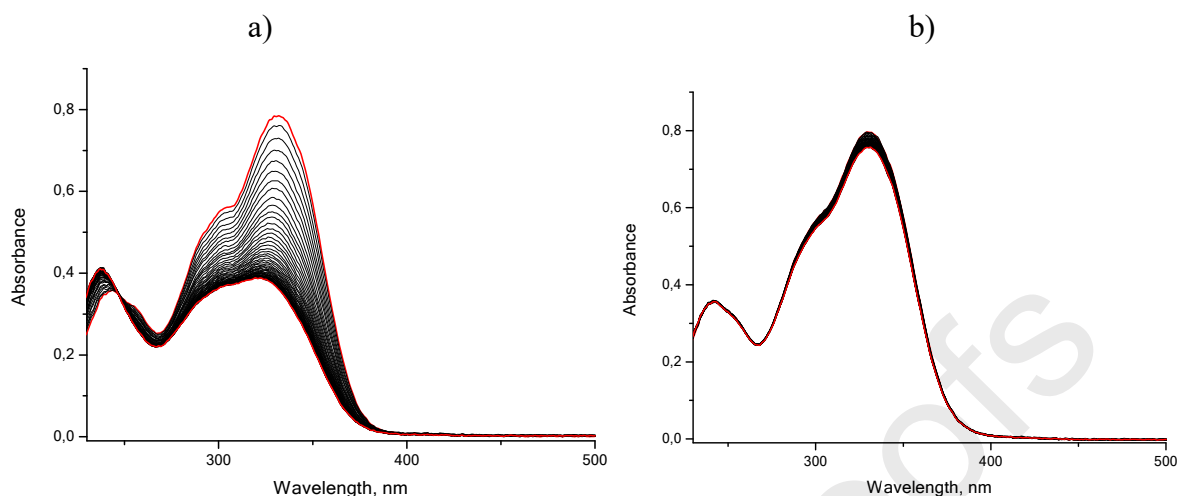


**Figure 1.** Spectral changes during photolysis of *E*-1 in acetonitrile (a) and water (b) with light  $\lambda = 365$  nm,  $C_{E-1} = 3 \cdot 10^{-5}$  M.

The absorption of *E*-1 and *E*-5 were simulated in ACN solvent using density functional theory (DFT) with the PBE0 [37] functional and the 6-311G(d,p) basis set. The absorption wavelengths ( $\lambda$  in nm) oscillator strengths ( $f$ ) are collected in Table S2 and S3 in ESI and also displayed in Figure S61 and S62 in ESI. The maximum absorption was calculated at 338 nm and 345 nm for the most stable isomer of *E*-5 and *E*-1, what is in excellent agreement with experiment (experimental  $\lambda_{\text{abs}} = 332$  nm and 330 nm, respectively). The HOMO and LUMO orbitals, shown in Figure 2 are largely delocalized on the whole conjugated skeleton of the molecule. Interestingly the *E*-*Z* isomerization induces some little changes in the absorption spectra similar to what was found in experiment, i.e. a decrease in the intensity and small blue-shift (Figure S62 in ESI).

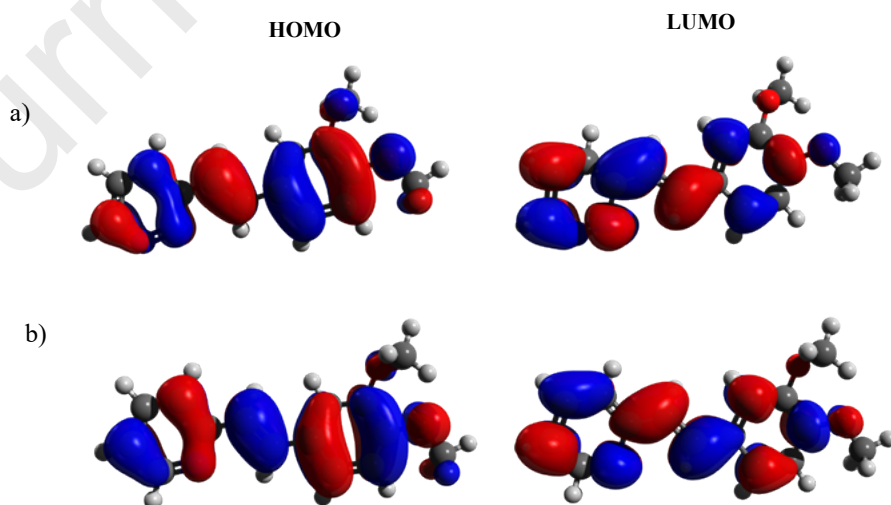
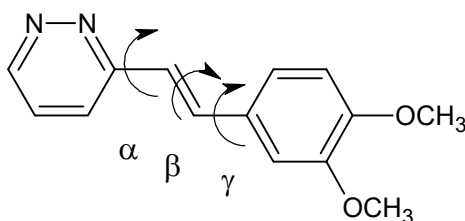


**Figure 2.** Molecular orbitals (HOMO and LUMO) implied in the maximum absorption excitation: a) *E*-1; b) *E*-5.

The conjugated chain connecting the heterocyclic units exhibit three partial double bonds (scheme 2). Therefore, 8 distinct isomers can be drawn and will be labeled with a sequence of three letters Z and/or E starting from the pyridine or pyridazine unit and indicating the approximate setting of the three dihedral angles  $\alpha$ ,  $\beta$  and  $\gamma$  as Z ( $0^\circ < \alpha < 90^\circ$ ) or E ( $90^\circ < \alpha < 180^\circ$ ), respectively (see for example the EEE isomer of compound *E-1* in Scheme 2).



**Scheme 2:** EEE isomer of compound *E-1*

The different isomers that can be formed from *E-1* and *E-5* were studied using DFT calculations (Tables S2 and S3 in ESI). Unambiguously the calculations show that ZEZ is the most stable isomer while the second more stable is ZEE. These results indicate that the *E* to *Z* isomerization around the double bond connecting the pyridine or pyridazine have a strong impact on the stability of the isomer while the *E* to *Z* around the double bond connecting the benzene ring have only a moderate influence on the stability of the isomer.

### **Photocycloaddition**

Prolonged irradiation of *E-1* – *E-5* with  $\lambda > 330$  nm resulted in more complex spectral changes depending on the solvent nature and the concentration of *E-1* – *E-5* used.

It was shown that irradiation of aqueous solutions of *E-1* – *E-4* with a concentration above  $2 \cdot 10^{-2}$  M leads to a decrease in the intensity of the long-wavelength absorption band in the spectral region 330-350 nm, which indicates a decrease in conjugation in the chromophoric system (Fig. 3a, Figs. S34-S42 in ESI). At the same time, a new blue-shifted band appeared at 270-280 nm, which is the characteristic absorption region of non-conjugated aromatic and heteroaromatic fragments. By analogy with [20], it can be assumed that during photolysis **1-4** undergo the [2+2] photocycloaddition reaction at the ethylene double bonds with the formation of the corresponding cyclobutane derivatives **1a-4a** (Scheme 1). It is interesting to note that the solubility of the resulting photolysis products in water is very low, so that during photolysis they precipitate out of solution (Fig. S41 in ESI). For this reason, a low-intensity peak of cyclobutane is observed on the HPLC chromatogram, while the peak of the starting compound constantly decreases during photolysis until it disappears (Fig. 3b).

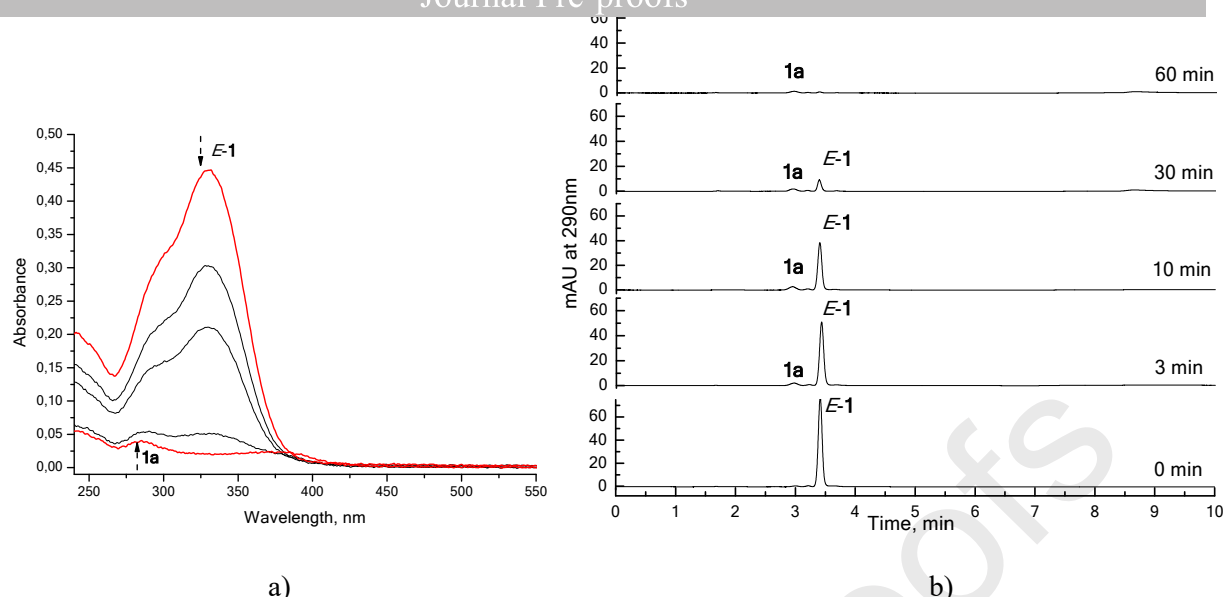


**Fig. 3** (a) Spectral changes and (b) HPLC chromatogram (eluent acetonitrile:water = 65:35) during photolysis of *E-1* ( $C_1 = 2 \cdot 10^{-2}$  M) in an aqueous solution with 365 nm light for 60 min. To measure the UV-Vis spectra, the solutions after photolysis were diluted to  $3 \cdot 10^{-5}$  M.

The formation of cyclobutane derivatives **1a-4a** was confirmed by NMR studies (Figs. 4, 5 and Figs. S6-S21 in ESI) and ESI-MS (Figs. S52-55 in ESI), and this [2+2] photocycloaddition reaction turned out to be regio- and stereoselective.

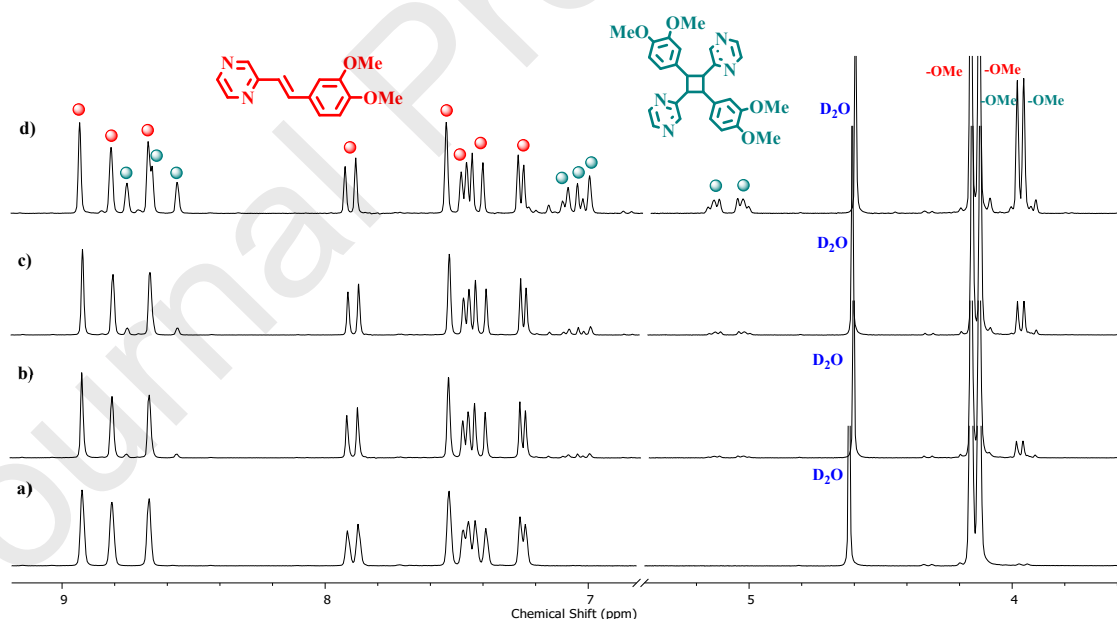


**Fig. 4** Fragments of <sup>1</sup>H NMR spectra (400 MHz) in 50% CD<sub>3</sub>CN / 50% D<sub>2</sub>O. Spectral changes during photolysis of *E-2* ( $C_2 = 8 \cdot 10^{-2}$  M) with light  $\lambda > 330$  nm for 0 min (a); 5 min (b); 10 min (c); 40 min (d).

As a result of the photoaddition reaction of compounds *E-1-E-4*, only one isomer of cyclobutanes **1a-4a** is formed out of eleven possible ones (Fig. 4). In addition, the signals of the protons of the cyclobutane ring appear in the form of a symmetric spin system AA'BB' with

vicinal coupling constants  $^3J_{ab} = ^3J_{a'b'} = 9.9$  and  $^4J_{ab} = ^4J_{a'b'} = 7.5$  Hz (Fig. 4). This also indicates the transoid geometry of the Ha and Hb protons in **2a**.

The mutual position of the substituents in the cyclobutane structure was established using two-dimensional NOESY NMR spectroscopy (Fig. 5 and Figs. S9, S13, S17, S21 in ESI). For example, in the structure of the isomer of cyclobutane **2a**, strong through-space interactions are observed between protons H-9, H-6, H-2 and protons of the cyclobutane ring, which means that these protons are located close to each other on the same side of the cyclobutane ring (Fig. 5).

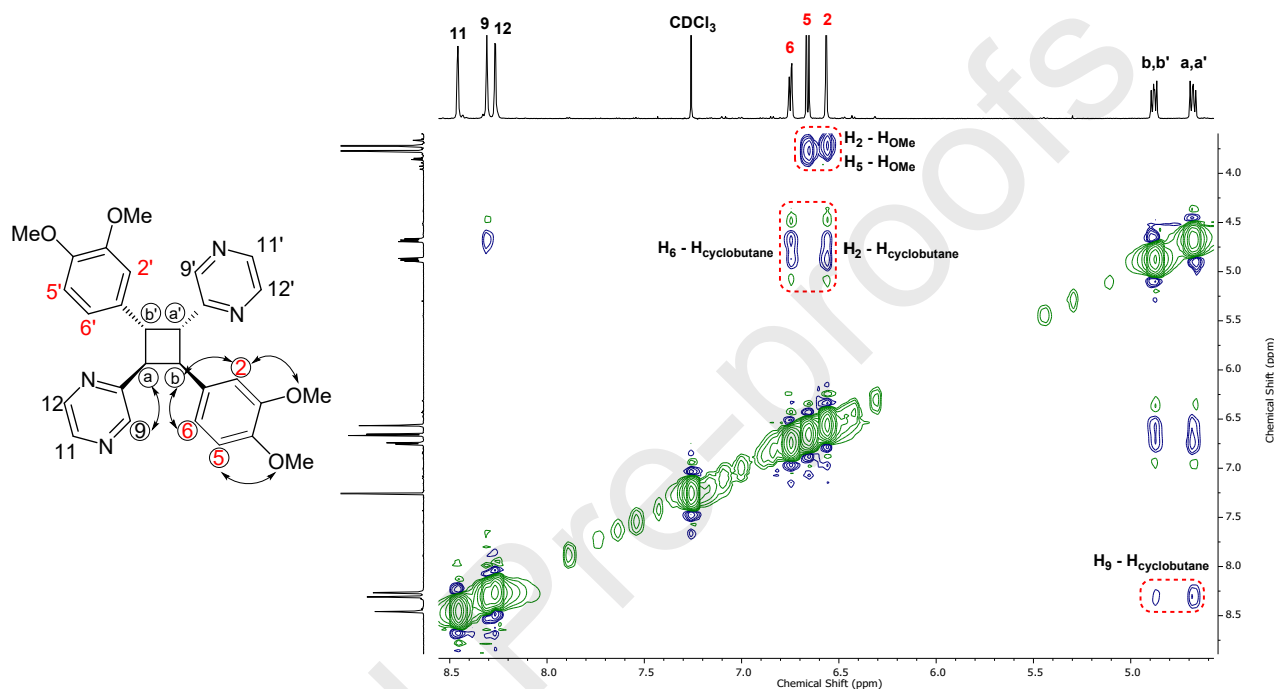


**Fig. 5** NOESY spectrum of **2a** ( $\text{CDCl}_3$ , 600 MHz)

A similar structure of cyclobutane derivatives with *head-to-tail* arrangement of heterocyclic and phenyl fragments was obtained for **1a**, **3a** and **4a** (Figs. S6-S21 in ESI).

In solid state the X-Ray analysis of **1a** and **3a** were performed (Figs. 6, S60 and Table S1 in ESI). The X-ray data demonstrated the similar structures of cyclobutanes produced from **1a** and **3a**.

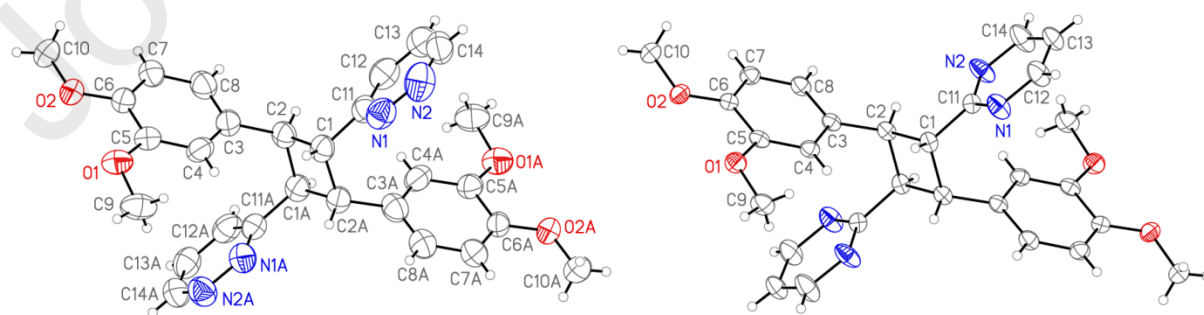


**Fig. 6** General view of crystal structures **1a** and **3a** in thermal ellipsoid representation for non-hydrogen atoms ( $p=50\%$ ), the atoms of the independent part are labeled. The minor disorder components in both structures are omitted for clarity.

For the photocycloaddition reaction to proceed with high regio- and stereoselectivity, the two reacting molecules must be appropriately pre-organized, forming dimers either in the ground state or in an excited state, that is, excimers [46–52]. From the quantum-chemical calculations, it could be also be seen that the isomers exhibit significant polarity. However the situation is contrasted either the compound contain a pyridine (*E-5*) or pyridazine (*E-1*) unit. The calculated dipole moment of *E-5* is found between 1.86 D and 4.75 D for the highest polar isomer (EZZ) (Table S2 in ESI). Interestingly the isomers of *E-1* show a much more pronounced polarity with values of the dipole moment going from 4.14 D to 8.93 D for the EZZ (Table S3 in ESI). A strong dipole moment could favor the formation of a complex through dipole-dipole interaction at the ground state before the [2+2] cycloaddition. The calculations results presented here on the monomer suggest that the complex dimer formation are more favored for *E-1* than for *E-5*.

We tested the possibility of self-organization of *E-1-E-4* into dimers or excimers, which could provide high regio- and stereoselectivity of photocycloaddition. For this purpose, we investigated the dependence of the spectral characteristics of aqueous solutions *E-1-E-4* on concentration. To detect the formation of dimers, we analyzed the changes in the absorption spectra of solutions of *E-1* of various concentrations from  $1 \cdot 10^{-5}$  M to  $8 \cdot 10^{-2}$  M in water, acetonitrile and a mixture water:acetonitrile = 1:1. In the absorption spectra of *E-1*, normalized at a wavelength of 242 nm, at concentrations above  $2 \cdot 10^{-2}$  M, a change in the shape of the spectra and their broadening were observed in water (Fig. 7A), and in a mixture water:acetonitrile = 1:1 (Fig. 7B), which may indicate the formation of dimers (*E-1*)<sub>2</sub> in the ground state. For acetonitrile solutions *E-1*, no change in the shape of the absorption was observed with increasing concentration (Fig. 7C), which indicates that dimers are not formed in this case. Fluorescence of *E-1* in water:acetonitrile = 1:1 is very weak, and the long-wavelength fluorescence that is characteristic of excimers was not observed in either acetonitrile or water for any concentration of *E-1* (Fig. S56-57). Most likely, the photocycloaddition reaction leading to the formation of **1a** in an aqueous solution or in a mixture water:acetonitrile = 1:1 proceeds through direct excitation of (*E-1*)<sub>2</sub> dimers formed in solutions with a high concentration of *E-1*.

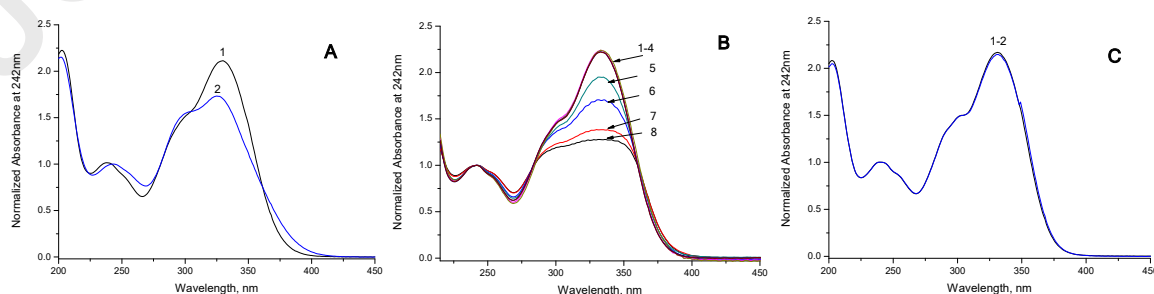


**Fig. 7** Absorption spectra of *E-1* normalized at 242 nm. (A)  $C_1 = 3.2 \cdot 10^{-4}$  M (1),  $6.4 \cdot 10^{-2}$  M (2), H<sub>2</sub>O, 20°C; (B)  $C_1 = 8 \cdot 10^{-5}$  M (1),  $8 \cdot 10^{-4}$  M (2),  $1 \cdot 10^{-2}$  M (3),  $2 \cdot 10^{-2}$  (4),  $4 \cdot 10^{-2}$  M (5),  $6 \cdot 10^{-2}$  M (6),

$7 \cdot 10^{-2}$  M (7),  $8 \cdot 10^{-2}$  M (8),  $\text{H}_2\text{O}:\text{MeCN}=1:1$ ,  $20^\circ\text{C}$ ; (C)  $C_1 = 8 \cdot 10^{-3}$  M (1),  $8 \cdot 10^{-2}$  M (2), MeCN,  $20^\circ\text{C}$ .

On the other hand, the formation of cycloadducts **1a-4a** was not detected in acetonitrile even at high concentrations of *E-1-E-4* up to  $8 \cdot 10^{-2}$  M (Fig.8), probably due to the fact that dimers of compounds *E-1-E-4* in acetonitrile are not formed.

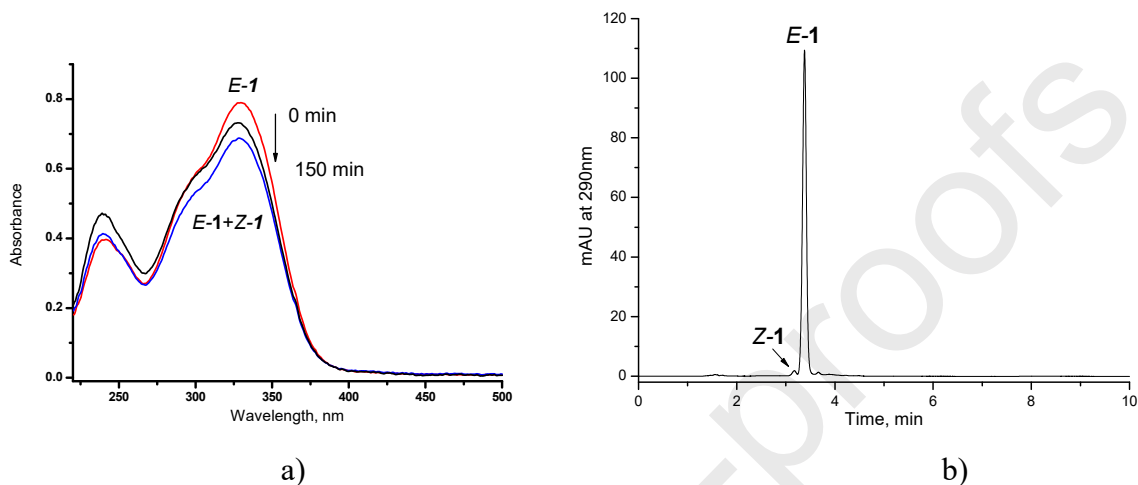


**Fig. 8** a) Spectral changes during photolysis of  $6 \cdot 10^{-2}$  M *E-1* in acetonitrile with 365 nm light for 150 min. To measure the spectra, the solutions after photolysis were diluted to  $3 \cdot 10^{-5}$  M; b) HPLC chromatogram of  $3 \cdot 10^{-5}$  M *E-1* after irradiation for 240 min with 365 nm light, eluent acetonitrile:water = 65:35.

Retro-photocycloaddition reaction of cyclobutanes **1a-4a** was observed in water upon irradiation with 313 nm light. HPLC analysis showed that, for example, after irradiation of a solution of cyclobutane **4a** in water with 313 nm light, a mixture of isomers *E-4* and *Z-4* was detected (Figs.9a-c and Figs. S49, S50). For **2a** and **4a**, the quantum yields of the retro-photocycloaddition reaction were determined (Table 1).

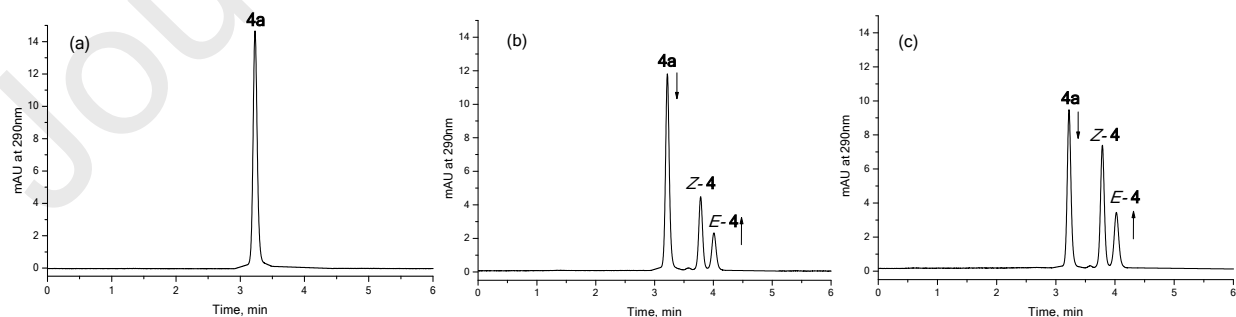


**Fig. 9** HPLC analysis of retro-photocycloaddition reaction of **4a** in  $\text{H}_2\text{O}$  upon irradiation with 313 nm light during 0 min (a); 60 min (b); 120 min (c), leading to the formation of *E-4* and *Z-4* isomers. Eluent MeCN: $\text{H}_2\text{O}$ =65:35.

### Electrocyclization

Prolonged irradiation of  $2 \cdot 10^{-5}$  M *E-1* in air saturated  $H_2O$  with  $\lambda > 330$  nm resulted in the appearance of the novel absorption band with maximum at 380 nm (Fig. 10) which can be assigned to heteroaromatic compound **1b** (Scheme 1) formed as a result of C-N oxidative photocyclization by analogy with 2-styrylquinolines studied earlier [53]. Indeed, the formation of C-N photocyclization product **5b** has been proven by NMR data (Fig. S56).

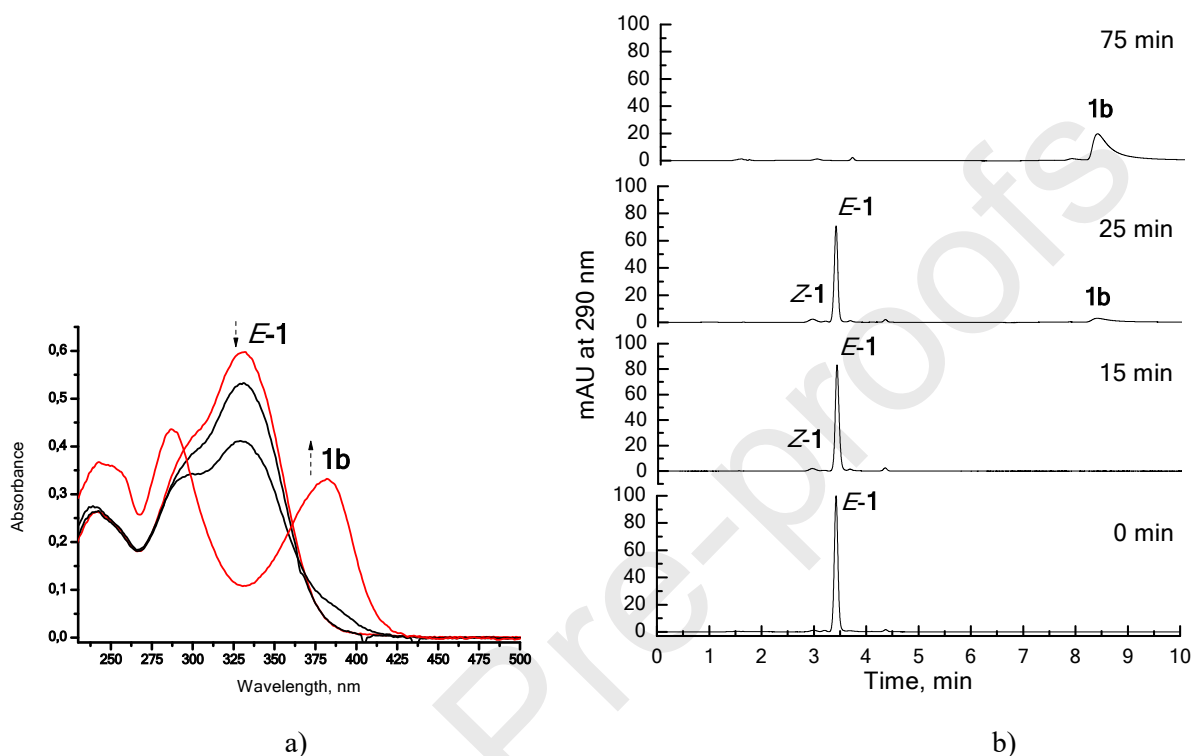


**Fig. 10** a) Spectral changes during photolysis of *E-1* in  $H_2O$  with light  $\lambda > 330$  nm for 75 min,  $C_1 = 2 \cdot 10^{-5}$  M; b) HPLC chromatogram of solution *E-1* showing a decrease in the concentration of *E-1* and an increase in the concentration of the electrocycle **1b** when irradiated with light  $\lambda > 330$  nm; eluent acetonitrile:water = 65:35.

Similar products of oxidative electrocyclization reaction were obtained upon irradiation with  $\lambda > 330$  nm of  $2 \cdot 10^{-5} \div 1 \cdot 10^{-3}$  M aqueous solutions *E-2-E-5*. It should be noted that at such concentrations, no photocycloaddition products **1a-4a** were formed. Apparently, dimers are not formed at low concentrations *E-1-E-4*, and for this reason the photocycloaddition reaction does not proceed under these conditions.

It was found that the direction of the photochemical reaction can be controlled by changing the composition of the solvent and the concentration of the compounds. For example, photolysis of  $3 \cdot 10^{-2}$  M *E-1* in a mixture water:acetonitrile = 1:1 leads to the simultaneous formation of cyclobutane **1a** and electrocyclic product **1b** (Scheme 1 and Fig. 10). The HPLC data showed that electrocycle **1b** was predominantly formed during photolysis and the ratio **1a:1b** = 1 : 2.5.

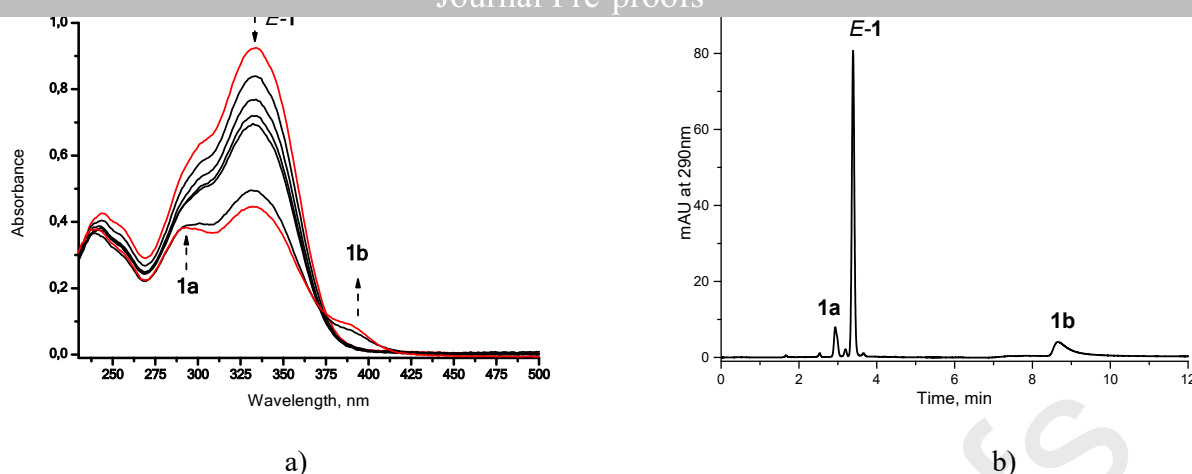


**Fig. 10** a) Spectral changes during photolysis of *E-1* in  $\text{H}_2\text{O}:\text{MeCN} = 1:1$  with 365 nm light for 250 min,  $C_1 = 3 \cdot 10^{-2}$  M. To measure the spectra, the solutions after photolysis were diluted to  $3 \cdot 10^{-5}$  M, b) HPLC chromatogram of the solution of *E-1* after irradiation with 365 nm light for 250 min; eluent acetonitrile:water = 65:35.

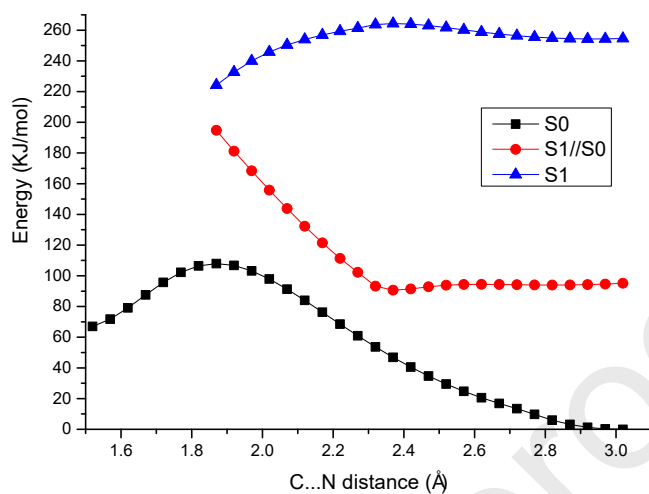
Thus, the concentration of the irradiated solution and the nature of the solvent can be changed to control the photochemical reaction. In aqueous solutions, an increase in the concentration of *E-1* - *E-4* leads to a shift in the photochemical reaction from electrocyclization products **1b** - **2b**, **5b** to cyclobutanes **1a** - **4a**. These results confirm our assumptions that the high regioselectivity of the cycloaddition reaction is mainly determined by the arrangement of stilbene molecules to the dimer at an olefin concentration of  $10^{-2}$  M or more. On the other hand, in acetonitrile, the main photochemical conversion of compounds *E-1-E-5* is the electrocyclization reaction with the formation of benzo[*c*]quinolizinium cation **5b** and its aza- analogs **1b-2b** in both dilute and concentrated solutions [19]. It should be noted that the photocycloaddition reaction was not observed for the pyridine derivative *E-5* in all solvents and at all concentrations used, most likely because the polarity of *E-5* is insufficient for pre-organization of *E-5* into dimers, which is not the case for compounds *E-1-E-4* containing two nitrogen atoms in heterocyclic moieties. Thus, heterocyclic moieties also affect the efficiency of photocyclization.

For deep analysis of the mechanisms of the photocyclization reaction the reaction pathway was optimized using the DFT and TD-DFT calculations by scanning the N...C distance starting from the ZZE isomer of heterostilbenes *E-1* and *E-5*. This procedure provides better precision than determination of the reaction path from the calculation of excitation energies using single-point TD-DFT and based on the ground states optimized geometries.

As seen in the Figure 11, the reaction proceeds through a transition state in ground state and the energies barriers for cyclization of *E-5* and *E-1* were found to be  $120.4 \text{ kJ}\cdot\text{mol}^{-1}$  ( $28.8 \text{ kcal}\cdot\text{mol}^{-1}$ ) and  $108.0 \text{ kJ}\cdot\text{mol}^{-1}$  ( $25.8 \text{ kcal}\cdot\text{mol}^{-1}$ ) respectively. These energies barriers values

hampere the thermal reaction and are consistent with no cyclization reaction in ground state as observed experimentally.

a)



b)

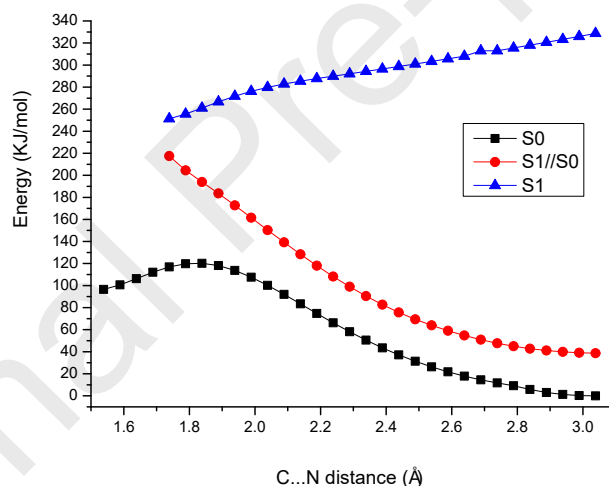


**Fig. 11** Potential energy surfaces of a) *E-1* and b) *E-5* along the C...N (distance of the two atoms that form a single bond by electrocyclization). Solid black line show energy of  $S_0$  state. Solid red line represent  $S_1$ - $S_0$  vertical energies calculated using the optimized  $S_1$  geometries. Blue line show energy of relaxed  $S_1$  state. Geometries are optimized by BPE0/6-311G(d,p) in ACN solvent using DFT and time-dependent DFT.

As shown in Figure 11 the photocyclization occurs at the  $S_1$  potential energy surface with a very small activation energy for *E-1*, which would occur easily. The excited molecule in the  $S_1$  evolves to a minimum obtained for a C...N distance of to 2.9 Å very close to the Franck-Condon region. From this minimum and by decreasing the C...N distance, a transition structure was found at 2.3775 Å (see Figure S63 in ESI) and confirmed by vibrational analysis. The energy barrier of 10  $\text{kJ}\cdot\text{mol}^{-1}$  is calculated at PBE0/6-311G(d,p) level. From the transition state, the  $S_1$  energy

decreases and a crossing point is found in which the C...N distance is about 1.9 Å and where efficient relaxation to the ground state is expected toward product or reactant.

Replacement of the pyrazidine (*E-1*) by a pyridine (*E-5*) group have an important effect on the excited state electrocyclic reaction. Indeed, no minimum and transition state could be located on the excited state PES for the compound *E-5*. In other word, after excitation of the molecule, the electrocyclization proceeds with no barrier and the system evolves until the conical intersection region.

In order to understand the difference in the photoreactivity between the excited cyclization reaction between *E-5* and *E-1* we analyzed the evolution of the LUMO orbital along the excited reaction pathway. During the electrocyclic reaction, the energy of this orbital is the result of several bonding and antibonding evolution and as a result its energy can increase or decrease.

In the first stage of the reaction, the energy of the LUMO of *E-1* increases and rapidly decreases when the conical intersection is reached. This energy profile similar to the energy of the S1 state and can be explain by the increase of the C-N bond length that causes an energy penalty of the LUMO (see Figure S64 in ESI). Once the transition state in excited state passed, the C-N bond length do not change significantly and the energy of the LUMO is then dominated by the development of the bonding character between the reactive N and carbon atoms.

By contrast the evolution of the LUMO of *E-5* shows quite different behavior and continuously decreases until the conical intersection, a similar evolution for the S1 energy. From this analysis it can be concluded that the S1 energy evolution is mainly driven by the bonding character of the LUMO.

The calculated absorption spectra of electrocyclic products **1b** and **5b** demonstrates good agreement between experimental and calculation data obtained in this paper (Figs. S65, S66 in ESI).

## Conclusion

We have illustrated a novel protocol in synthetic organic photochemistry to tune the direction of phototransformation aimed to prepare the required photoproduct in native condition. Stilbene derivatives *E-1-E-5* can participate into parallel reactions of *E-Z*-photoisomerization followed by electrocyclization and intermolecular [2+2] - photocycloaddition with the formation of tetrasubstituted cyclobutane. The photophysical processes such as luminescence can compete with the photochemical transformation. We found that water effectively stabilizes the polar excited state, increasing the probability of photochemical conversion over emission. Photolysis of *E-1-E-5* in a dilute aqueous solution (at an olefin concentration below  $10^{-2}$ M) leads to a regioselective electrocyclic reaction through the formation of a novel C-N bond with the formation of

benzo[c]quinolinium cation **5D** and its aza-analogues **1D-2D**. In a solution of *E-1-E-4* with a concentration of more than  $10^{-2}$  M, the spatial arrangement of stilbene molecules in a *head-to-tail* orientation provides a regio- and stereoselective photocycloaddition reaction, which gives only one isomer of cyclobutane in a sufficiently high yield (up to 57%). For the organization of stilbene molecules into dimers, their polarity is important. Thus, the pyridine derivative *E-5* is not capable of dimerization; however, stilbenes *E-1-E-4* with two nitrogen atoms in the heterocyclic ring are able to form dimers. The mild reaction conditions and the absence of additives facilitate the reaction. This work provides a convenient and gentle method for producing cyclobutanes.

### **CRediT authorship contribution statement**

Alina E. Saifutiarova: Investigation, Validate, Visualization, Writing- Original draft preparation. Yury V. Fedorov: Methodology, Formal analysis, Writing- Reviewing and Editing. François Maurel: Quantum-Chemical Calculations. Elena N. Gulakova: Conceptualization, Investigation. Valentina A. Karnoukhova: Investigation. Olga A. Fedorova: Methodology, Formal analysis, Conceptualization, Writing- Original draft preparation, Writing- Reviewing and Editing.

### **Declaration of Competing Interest**

The authors declare that they have no known competing financial interests or personal relationships that could have appeared to influence the work reported in this paper.

### **Acknowledgment**

This work was supported by the Russian Foundation for Basic Research (project no. 19-53-18010). The use of equipment from the Center of Collective Facilities of National Research Center «Kurchatov Institute» (project no. № 19-73-20187) (X-ray analysis) is gratefully acknowledged. The NMR spectra were recorded, and elemental analyses were performed, using the facilities of the Molecular Structure Research Center at the Nesmeyanov Institute of Organoelement Compounds, Russian Academy of Sciences, under support by the Ministry of Science and Higher Education of the Russian Federation.

### **References**

- [1] J.C. Namyslo, D.E. Kaufmann, The application of cyclobutane derivatives in organic synthesis, *Chemical Reviews*. 103 (2003) 1485–1537. <https://doi.org/10.1021/CR010010Y>.
- [2] N. Hoffmann, Photochemical reactions as key steps in organic synthesis, *Chemical Reviews*. 108 (2008) 1052–1103. <https://doi.org/10.1021/CR0680336>.
- [3] E. Gravel, E. Poupon, Biogenesis and biomimetic chemistry: Can complex natural products be assembled spontaneously?, *European Journal of Organic Chemistry*. (2008) 27–42. <https://doi.org/10.1002/EJOC.200700331>.
- [4] A.A.Q. Al-Khdhairawi, P. Krishnan, C.W. Mai, F.F.L. Chung, C.O. Leong, K.T. Yong, K.W. Chong, Y.Y. Low, T.S. Kam, K.H. Lim, A Bis-benzopyrroloisoquinoline Alkaloid Incorporating a Cyclobutane Core and a Chlorophenanthroindolizidine Alkaloid with Cytotoxic Activity from *Ficus fistulosa* var. *tengerensis*, *Journal of Natural Products*. 80

- (2017) 2734–2740. <https://doi.org/10.1021/ACS.JNATPROD.7B00500>.
- [5] V. M. Dembitsky, Naturally occurring bioactive Cyclobutane-containing (CBC) alkaloids in fungi, fungal endophytes, and plants. *Phytomedicine*. 21(12) (2014) 1559–1581. <https://doi.org/10.1016/j.phymed.2014.07.005>.
- [6] P. Koparir, M. Karaarslan, C.O.- Phosphorus, undefined Sulfur, undefined and, undefined 2011, Synthesis and in-vitro antimicrobial activity of novel aminophosphinic acids containing cyclobutane and 1, 3-thiazole, Taylor & Francis. 186 (2011) 2368–2376. <https://doi.org/10.1080/10426507.2011.604660>.
- [7] A. Çukurovali, I. Yilmaz, H. Özmen, Antimicrobial activity studies of the metal complexes derived from substituted cyclobutane substituted thiazole Schiff base ligands, *Transition Metal Chemistry*. 26 (2001) 619–624. <https://doi.org/10.1023/A:1012006404144>.
- [8] J. Menezes, Natural dimers of coumarin, chalcones, and resveratrol and the link between structure and pharmacology. 182 (2019) 111637. <https://doi.org/10.1016/j.ejmech.2019.111637>.
- [9] S Kölsch, S., Ihmels, H., Mattay, J., Sewald, N., & Patrick, B. O. Reversible photoswitching of the DNA-binding properties of styrylquinolinium derivatives through photochromic [2+2] cycloaddition and cycloreversion. *Beilstein journal of organic chemistry*. 16(1) (2020) 111–124. <https://doi.org/10.3762/bjoc.16.13>.
- [10] Hans-Albert Brunea, Tony Debaerdemaekere, Uwe Giintherb, Giinther Schmidtberg and Ulrich Zieglerb, Photochemistry of fluoro- and chloro-substituted trans-stilbene-4-carboxylic-acids and their derivatives in the crystalline phase. *Photochem. Photobiol. A: Chem.* 83 (1994) 113–128. [https://doi.org/10.1016/1010-6030\(94\)03818-X](https://doi.org/10.1016/1010-6030(94)03818-X).
- [11] F.-L. Hu, Y. Mi, C. Zhu, B.F. Abrahams, P. Braunstein, J.-P. Lang, Stereoselective Solid-State Synthesis of Substituted Cyclobutanes Assisted by Pseudorotaxane-like MOFs, *Angewandte Chemie*. 130 (2018) 12878–12883. <https://doi.org/10.1002/ANGE.201806076>.
- [12] E.V. Tulyakova, O.A. Fedorova, Yu V. Fedorov, A.V. Anisimov, [2 + 2]-Photocycloaddition reaction of self-assembled crown-containing 2-styrylpyridinium perchlorate in a solid state. *Journal of Photochemistry and Photobiology A: Chemistry*. 200 (1) (2008) 90–95. <https://doi.org/10.1016/j.jphotochem.2008.02.023>.
- [13] B. Bibal, C. Mongin, D. M. Bassani, Template Effects and Supramolecular Control of Photoreactions in Solution. *Chem. Soc. Rev.* 43 (2014) 4179–4198. <https://doi.org/10.1039/C3CS60366K>.
- [14] V. Ramamurthy, J.S.-C. reviews, undefined 2016, Supramolecular photochemistry as a potential synthetic tool: photocycloaddition, ACS Publications. 116 (2016) 9914–9993. <https://doi.org/10.1021/acs.chemrev.6b00040>.
- [15] N. Sinha, F.H.-A. of chemical research, undefined 2017, Metallosupramolecular architectures obtained from poly-N-heterocyclic carbene ligands, ACS Publications. 50 (2017) 11. <https://doi.org/10.1021/acs.accounts.7b00158>.
- [16] M. Pattabiraman, A. Natarajan, R. Kaliappan, Magueb, J. T. Ramamurthy, V, Template Directed Photodimerization of Trans-1,2-bis(n-pyridyl)ethylenes and Stilbazoles in Water. *Chem. Commun.* (2005) 4542–4544. <https://doi.org/10.1039/B508458J>.
- [17] X. Tang, Z. Huang, H. Chen, Y. Kang, J.F. Xu, X. Zhang, Supramolecularly Catalyzed Polymerization: From Consecutive Dimerization to Polymerization, *Angewandte Chemie - International Edition*. 57 (2018) 8545–8549. <https://doi.org/10.1002/ANIE.201803749>.
- [18] D. Berdnikova, T. Aliyev, S. Delbaere, Yu. Fedorov, Jonusauskas Gediminas, V. Novikov, AA. Pavlov, A Peregudov, N. Shepel', F. Zubkov, O. Fedorova, Regio- and stereoselective [2+2] photocycloaddition in Ba<sup>2+</sup> templated supramolecular dimers of styryl-derivatized aza-heterocycles. *Dyes and Pigments*. 139 (2017) 397–402. <https://doi.org/10.1016/j.dyepig.2016.11.053>.
- [19] O. Fedorova, Yu. Fedorov, E. Gulakova, N. Schepel, M. Alfimov, U. Goli, J. Saltiel, Supramolecular photochemical synthesis of an unsymmetrical cyclobutane. *Photochemical and Photobiological Sciences*. 6 (10) (2007) 1097–1105.

- <https://doi.org/10.1039/B707093D>.
- [20] O. A. Fedorova, A. E. Saifutiarova, E. N. Gulakova, E. O. Guskova, T. M. Aliyev, N. E. Shepel, Y. V. Fedorov, The regioselective [2+ 2] photocycloaddition reaction of 2-(3, 4-dimethoxystyryl) quinoxaline in solution. *Photochemical & Photobiological Sciences*. 18(9) (2019) 2208–2215. <https://doi.org/10.1039/c9pp00028c>.
- [21] R. Kaliappan, L. S. Kaanumalle, A. Natarajan, V. Ramamurthy, Templating Photodimerization of Stilbazoles with Water-Soluble Calixarenes. *Photochem. Photobiol. Sci.* 5 (2006) 925–930. <https://doi.org/10.1039/B606658E>.
- [22] M. Yoshizawa, Y. Takeyama, T. Okano, M. Fujita, Cavity-directed synthesis within a self-assembled coordination cage: Highly selective cross-photodimerization of olefins, ACS Publications. (2003). <https://doi.org/10.1021/ja020718>.
- [23] Y. Nishioka, T. Yamaguchi, M. Yoshizawa, M. Fujita, Unusual [2+4] and [2+2] cycloadditions of arenes in the confined cavity of self-assembled cages, *Journal of the American Chemical Society*. 129 (2007) 7000–7001. <https://doi.org/10.1021/JA071591X>.
- [24] G.M.J. Schmidt, Photodimerization in the solid state, *Pure and Applied Chemistry*. 27 (1971) 647–678. <https://doi.org/10.1351/PAC197127040647/HTML>.
- [25] J. Saltiel, Stilbenes: Applications in Chemistry, Life Sciences and Materials Science, *Journal of the American Chemical Society*. 132 (2010) 9221–9222. <https://doi.org/10.1021/JA104338D>.
- [26] T.M. Aliyev, D. V. Berdnikova, O.A. Fedorova, E.N. Gulakova, C. Stremmel, H. Ihmels, Regiospecific Photocyclization of Mono- and Bis-Styryl-Substituted N-Heterocycles: A Synthesis of DNA-Binding Benzo[c]quinolininium Derivatives, *Journal of Organic Chemistry*. 81 (2016) 9075–9085. <https://doi.org/10.1021/ACS.JOC.6B01695>.
- [27] D.F. Eaton, Reference Materials for Fluorescence Measurement, *Pure and Applied Chemistry*. 60 (1988) 1107–1114. <https://doi.org/10.1351/PAC198860071107/HTML>.
- [28] C.L. Renschler, L.A. Harrah, Determination of Quantum Yields of Fluorescence by Optimizing the Fluorescence Intensity, *Analytical Chemistry*. 55 (1983) 798–800. <https://doi.org/10.1021/ac00255a050>.
- [29] D. V. Berdnikova, T.M. Aliyev, T. Paululat, Y. V. Fedorov, O.A. Fedorova, H. Ihmels, DNA - Ligand interactions gained and lost: Light-induced ligand redistribution in a supramolecular cascade, *Chemical Communications*. 51 (2015) 4906–4909. <https://doi.org/10.1039/c5cc01025j>.
- [30] R.D. Svetogorov, P. V. Dorovatovskii, V.A. Lazarenko, Belok/XSA Diffraction Beamline for Studying Crystalline Samples at Kurchatov Synchrotron Radiation Source, *Crystal Research and Technology*. 55 (2020). <https://doi.org/10.1002/CRAT.201900184>.
- [31] W. Kabsch, Biological Crystallography, *Research Papers Acta Cryst.* 66 (2010) 125–132. <https://doi.org/10.1107/S0907444909047337>.
- [32] Y. Liu, C. He, Y. Tang, G.H. Imler, D.A. Parrish, J.M. Shreeve, Tetrazolyl and dinitromethyl groups with 1,2,3-triazole lead to polyazole energetic materials, *Dalton Transactions*. 48 (2019) 3237–3242. <https://doi.org/10.1039/C8DT05071F>.
- [33] L. Krause, R. Herbst-Irmer, G.M. Sheldrick, D. Stalke, Comparison of silver and molybdenum microfocus X-ray sources for single-crystal structure determination, *J. Appl. Cryst.* 48 (2015) 3–10. <https://doi.org/10.1107/S1600576714022985>.
- [34] G.M. Sheldrick, SHELXT - Integrated space-group and crystal-structure determination, *Acta Crystallographica Section A: Foundations of Crystallography*. 71 (2015) 3–8. <https://doi.org/10.1107/S2053273314026370>.
- [35] G.M. Sheldrick, Crystal structure refinement with SHELXL, *Acta Crystallographica Section C: Structural Chemistry*. 71 (2015) 3–8. <https://doi.org/10.1107/S2053229614024218>.
- [36] M. J. Frisch, G. W. Trucks, H. B. Schlegel, G. E. Scuseria, M. A. Robb, J. R. Cheeseman, G. Scalmani, V. Barone, G. A. Petersson, H. Nakatsuji, X. Li, M. Caricato, A. V. Marenich, J. Bloino, B. G. Janesko, R. Gomperts, B. Mennucci, H. P. Hratchian, J. V. Ortiz, A. F. Izmaylov, J. L. Sonnenberg, D. Williams-Young, F. Ding, F. Lipparini, F. Egidi, J. Goings,

- B. Peng, A. Petrone, I. Henderson, D. Kanasingne, V. G. Zakrzewski, J. Gao, N. Rega, G. Zheng, W. Liang, M. Hada, M. Ehara, K. Toyota, R. Fukuda, J. Hasegawa, M. Ishida, T. Nakajima, Y. Honda, O. Kitao, H. Nakai, T. Vreven, K. Throssell, J. A. Montgomery, Jr., J. E. Peralta, F. Ogliaro, M. J. Bearpark, J. J. Heyd, E. N. Brothers, K. N. Kudin, V. N. Staroverov, T. A. Keith, R. Kobayashi, J. Normand, K. Raghavachari, A. P. Rendell, J. C. Burant, S. S. Iyengar, J. Tomasi, M. Cossi, J. M. Millam, M. Klene, C. Adamo, R. Cammi, J. W. Ochterski, R. L. Martin, K. Morokuma, O. Farkas, J. B. Foresman, and D. J. Fox, Gaussian, Inc., Wallingford CT, 2016.
- [37] C. Adamo, V. Barone Toward reliable density functional methods without adjustable parameters: The PBE0 model, *J. Chem. Phys.*, 110 (1999) 6158-69. <https://doi.org/10.1063/1.478522>.
- [38] S. Hirata and M. Head-Gordon, Time-dependent density functional theory within the Tamm-Dancoff approximation, *Chem. Phys. Lett.*, (1999), 314, 291-299. [https://doi.org/10.1016/S0009-2614\(99\)01149-5](https://doi.org/10.1016/S0009-2614(99)01149-5).
- [39] Y. Zhao, D.G. Truhlar, Y. Zhao, D G Truhlar, The M06 suite of density functionals for main group thermochemistry, thermochemical kinetics, noncovalent interactions, excited states, and transition elements: two new functionals and systematic testing of four M06-class functionals and 12 other functionals, *Theoretical Chemistry Accounts* 2007 120:1. 120 (2007) 215-241. <https://doi.org/10.1007/S00214-007-0310-X>.
- [40] J. Da Chai, M. Head-Gordon, Long-range corrected hybrid density functionals with damped atom-atom dispersion corrections, *Physical Chemistry Chemical Physics*. 10 (2008) 6615-6620. <https://doi.org/10.1039/B810189B>.
- [41] T. Yanai, D.P. Tew, N.C. Handy, A new hybrid exchange-correlation functional using the Coulomb-attenuating method (CAM-B3LYP), *Chemical Physics Letters*. 393 (2004) 51-57. <https://doi.org/10.1016/J.CPLETT.2004.06.011>.
- [42] N.M. O'Boyle, A.L. Tenderholt, K.M. Langner, cclib: A library for package-independent computational chemistry algorithms, *Journal of Computational Chemistry*. 29 (2008) 839-845. <https://doi.org/10.1002/JCC.20823>.
- [43] S.F. Boys, F. Bernardi, The calculation of small molecular interactions by the differences of separate total energies. Some procedures with reduced errors, *Mol. Phys.* 19 (2006) 553-566. <https://doi.org/10.1080/00268977000101561>.
- [44] G. Scalmani, M.J. Frisch, Continuous surface charge polarizable continuum models of solvation. I. General formalism, *The Journal of Chemical Physics*. 132 (2010) 114110. <https://doi.org/10.1063/1.3359469>.
- [45] T.L. (Thomas L. Gilchrist, *Heterocyclic chemistry / T.L. Gilchrist*, (1992) 1-287.
- [46] M. (Michael) Gordon, W.R. Ware, *The exciplex*, (1975) 372.
- [47] N. Mataga, Development of exciplex chemistry: Some fundamental aspects, *Pure and Applied Chemistry*. 69 (1997) 729-734. <https://doi.org/10.1351/PAC199769040729/HTML>.
- [48] R.A. Caldwell, D. Creed, Exciplex Intermediates in [2 + 2] Photocycloadditions, *Accounts of Chemical Research*. 13 (1980) 45-50. <https://doi.org/10.1021/AR50146A003>.
- [49] R.A. Caldwell, L. Smith, Photocycloaddition of 9-Cyanophenanthrene to Substituted  $\beta$ -Methylstyrenes. Obligatory Exciplex Intermediate, *Journal of the American Chemical Society*. 96 (1974) 2994-2996. <https://doi.org/10.1021/JA00816A055>.
- [50] R.A. Caldwell, N.I. Ghali, C.K. Chien, D. DeMarco, L. Smith, Photocycloaddition of  $\beta$ -Methylstyrenes to Some 9-Cyanophenanthrenes. Chemical Consequences of Exciplex Formation, *Journal of the American Chemical Society*. 100 (1978) 2857-2863. <https://doi.org/10.1021/JA00477A047>.
- [51] Y. Yabuno, Y. Hiraga, R. Takagi, M. Abe, Concentration and Temperature Dependency of Regio-and Stereoselectivity in a Photochemical Cycloaddition Reaction (the Paternò-Büchi Reaction): Origin, ACS Publications. 133 (2011) 44. <https://doi.org/10.1021/ja1088524>.
- [52] H. Maeda, H. Takenaka, K. Mizuno, Intermolecular hydrogen bonding controlled

- stereoselective photocycloaddition of vinyl ethers to 1-cyanonaphthalenes, *Photochem. Photobiol. Sci.* 15 (2016) 1385–1392. <https://doi.org/10.1039/C6PP00281A>.
- [53] E.N. Gulakova, D. V. Berdnikova, T.M. Aliyev, Y. V. Fedorov, I.A. Godovikov, O.A. Fedorova, Regiospecific C-N photocyclization of 2-styrylquinolines, *Journal of Organic Chemistry*. 79 (2014) 5533–5537. <https://doi.org/10.1021/JO500696N>.

We have developed a visible light promoted reaction of intermolecular [2 + 2] cycloaddition of heterostilbene.

The efficiency of intermolecular [2 + 2] cycloaddition depends on the nature of the heterocyclic residue and the concentration of heterostilbenes.

Photolysis of heterostilbenes in a dilute aqueous solution (at an olefin concentration below  $10^{-2}$ M) leads to a regioselective electrocyclic reaction

In a solution of heterostilbenes with a concentration of more than  $10^{-2}$  M, the spatial arrangement of stilbene molecules in a head-to-tail orientation provides a regio- and stereoselective photocycloaddition reaction, which gives only one isomer of cyclobutane in a sufficiently high yield (up to 57%).

This work provides a convenient and gentle method for controlling the direction of photochemical transformations of heterostilbenes to obtain cyclobutanes or heteroaromatic cations.

### **Highly regioselective and stereoselective photodimerization of azine-containing stilbenes in neat condition: An efficient synthesis of novel cyclobutanes with heterocyclic substituents**

Alina E. Saifutiarova, Elena N. Gulakova, Yuri V. Fedorov, Valentina A. Karnoukhova, Olga A. Fedorova

